Isochronous sets in smooth and non-smooth mechanical oscillators

Aasifa Rounak
Indian Institute of Technology Madras
Sayan Gupta (sayan@iitm.ac.in)
Indian Institute of Technology Madras https://orcid.org/0000-0002-0970-3795

Research Article

Keywords: Isochrons, patterns, stochasticity, Non-smooth systems. Van der Pol oscillator, stick-slip belt friction oscillator

Posted Date: February 15th, 2022

DOI: https://doi.org/10.21203/rs.3.rs-1212827/v1

Nonlinear Dynamics manuscript No.
(will be inserted by the editor)

Isochronous sets in smooth and non-smooth mechanical oscillators

Aasifa Rounak · Sayan Gupta

Received: date / Accepted: date

Abstract This work aims at characterizing the patterns of iso-phases of periodic and noisy oscillations of smooth and non-smooth dynamical systems in the phase space. The values of asymptotic phases reached starting from various initial conditions form patterns in the basins of attraction in the phase space. Even though the phase of system's oscillations turn out to be functions of the phase of forcing for externally excited systems, for higher periodic oscillations some patterns or foliations within their basins are seen. For periodic oscillations, isophases coincide with the isochrons. For irregular oscillations, a notion of regularity of oscillations has been introduced and the sensitivity of the system to external forcing has been computed. For stable periodic oscillations of autonomous kind, in the presence of noise the extent of phase diffusion is observed to be orders higher than the diffusion in amplitude. For noisy forced oscillations, the phase is locked onto the deterministic phase with marginal dislocations within a limit ϵ dependent on the intensity of noise. This work deals with the above notions of iso-phases in the context of a Van der Pol and an autonomous stick-slip belt friction oscillator.

Keywords Isochrons · patterns · stochasticity · Non-smooth systems · Van der Pol oscillator · stick-slip belt friction oscillator

Aasifa Rounak
Department of Applied Mechanics
Indian Institute of Technology, Madras
Chennai, Tamil Nadu- 600036
E-mail: aasifa.rounak@gmail.com

Sayan Gupta
Department of Applied Mechanics
Also, Complex Systems and Dynamics Group,
Indian Institute of Technology, Madras
Chennai, Tamil Nadu
E-mail: sayan@iitm.ac.in

1 Introduction

Tracking the phase observable of dynamical systems provides insights into its dynamics. The dynamics can be studied in some autonomous systems by reducing the functional form of the governing equation to an expression that describes the shift in phases on account of perturbations to the limit cycle. This approach is known as phase reduction and is used to analyse autonomous dynamical systems in a lower dimensional space. This lower-dimensional representation of an oscillator's dynamics can help in visualizing important dynamical aspects such as regularity and sensitivity to forcing and noise [1,2]. The study of phase reduction approach also provides a systematic method for analyzing synchronization in phases in dynamical systems [3,4]. Synchronization can be treated as an appearance of a relation between functionals of two processes due to interaction and was described as early as the 17th century by Huygens, where synchronization had the connotation of locking of phases ϕ_1, ϕ_2, where $n\phi_1 - m\phi_2 = q$, where $m, n \in \mathcal{I}, q \in \mathcal{R}$. Coupled oscillators interact via mutual adjustment of their amplitudes and phases. When this coupling is weak, amplitudes of oscillations are relatively constant and the interactions could be described by phase models. However, [5] states that the phases of periodically forced models are not free in terms of existence of a zero Lyapunov function that corresponds to phase shift, and thus cannot be adjusted by small coupling.

The emphasis of this study is however to gain understanding on the physics of the behaviour of uncoupled dynamical systems, first for deterministic cases and also when subjected to noisy perturbations. To do so, phases in stochastic attractors are defined. For oscillatory time responses in noisy dynamical systems, analytical and numerical investigations to introduce a notion of isophases of oscillations and the system's sensitivity to external forcing have been proposed [6]. The asymptotic phases attained by trajectories starting in the basin of attraction of respective attractors in a dynamical system are examined. While phase is a fundamental concept, it has multiple definitions in literature that may lead to contradictory interpretations. A quantitative notion of phase can be assigned to every point in a trajectory traversing a limit cycle. Even though the phase of system's oscillations turn out to be functions of the phase of forcing for externally excited systems, for higher periodic oscillations some patterns or foliations within their basins have been seen [1]. These foliations in the basin of attraction, called isochrons, are described next. For periodic oscillations, "iso"-phases, or locus of points with similar phases, coincide with the isochrons, where the return times are always equal.

To define an isochron, one needs to understand the concept of a level set. A level set of a real valued function f of n variables $x_1, ..., x_n$, is a set of the form-

$$L_c(f) = \{(x_1, ..., x_n) | f(x_1, ..., x_n) = c\},$$

where the function takes a constant value of c. Closed form functions of phases in terms of state variables are technically known as the *phase function's level sets* [6]. The set of initial conditions in the basins of attraction of the attractor that lead to the trajectories asymptotically converging to the same phase are called iso-phases. Iso-phases can be defined as hyper-surfaces in the state space that contain the

initial conditions, starting from which, the return times of the trajectories to the attractor are almost equal. There have been fierce debates on the methodologies of defining the isophases. The most widely used method for nonlinear data analysis is the Hilbert transform method [7]. The complex plane in which the trajectory is analysed comprises of the analytic signal constructed from the original trajectory and its Hilbert transform. To get physically meaningful outputs, it is necessary to transform the signal that is being analysed to a rotational trajectory centered around the origin in the complex plane. Any multi-component or chaotic signal when transformed to a complex signal can be seen to have multiple centers of rotation, often not around the origin. Thus the representation of phase is multiply defined over such orbits [8]. The second approach involves constructing isophases as Poincaré sections with almost similar mean first return times to these sections [6] and using the argument of complex eigenfunction of the backward density evolution operator with the smallest real part of the eigenvalue [9]. However this approach has been largely debated [10, 11]. A third phase description, applicable to one-dimensional stochastic oscillators depends on the description of the invariant probability density [12]. For stable periodic oscillations of autonomous kind, in the presence of continuous stochastic perturbations, the extent of diffusion in phase of the points with similar return times is observed to be orders of magnitude higher than the diffusion in amplitude. There can be extrinsic fluctuations in a dynamical system that can perturb its trajectories from a stable invariant set $\mathcal{A}$ to undergo large excursions, directing it to the domain of another co-existing attractor or making the solution converge on to the same attractor but with a different phase. Such phenomena in phase dynamics have been studied under the context of phase transfers [2].Periodic oscillations can be characterized by the amplitude, frequency (or frequency spectrum) and phase. Several strategies proposed to control each of these characteristics have been discussed in [13]. In many of these studies, the objective of designing the control algorithm is to drive an oscillatory system to track the phase of the reference trajectory [14]. One such technique to track shifts in phase is known in literature as the phase response curve. Small perturbations can dislodge a trajectory from its stable oscillatory state and eventually as the perturbation dies off, the trajectory could asymptotically converge onto the same attractor but with a different phase. A phase response curve (PRC) is the plot depicting the transient change in the cycle period of an oscillator induced by a perturbation against the phase at which the perturbation is recieved. The concept of phase response curves have proved to be crucial for analyses and modeling of oscillatory dynamics of various applications [15–17]. This study primarily focuses on describing phases in terms of isochrons and their phase responses to perturbations or external forcing. In the following paragraphs, these concepts are explained in greater detail.

Isochrons as mentioned earlier can be formally defined as the locus of initial conditions in the state space that when evolved, have the steady state that exhibit the same phase of oscillation of the attractor. This concept was introduced by [4]. Guckenheimer *et. al* formalized the definition of an isochron as the stable manifold of the time map, T_Γ, of a given point, say γ, on the periodic orbit Γ [15]. A phase variable can be mapped to the time along the limit-cycle Γ, with any point marked on the cycle to have a zero phase, relative to the period of oscillation. From such a representation, the oscillator's phase can be used as effective one-dimensional

descriptors of higher dimensional dynamics, particularly for excited or coupled systems. As discussed, phases can be assigned to asymptotic responses of any trajectory beginning from a point in the state space. It has been observed to lead to a regular pattern in the state space. The isochrons of an autonomous system containing a $n-$dimensional periodic orbit Γ define a set of $(n-1)$ dimensional smooth manifolds that populate its n-dimensional basin of attraction. For forced systems with periodic attractors, the frequencies of such oscillations of the system get entrained alongwith the phase of forcing [18,19].

In the context of limit cycle oscillations, evolution of all trajectories with initial condition $x(0)$ lying within the basin of attraction of the limit cycle ends up at the limit cycle. In other words, there exists a point $x^{lc}(0)$ on the limit cycle such that $|x(t) - x^{lc}(t)| \to 0$ as $t \to \infty$. Then one can define the phase at $x(0)$ as $\phi(x(0)) = \phi(x^{lc}(0))$. Thus one attributes the phase of the point on the limit cycle, to which trajectories emanating from the given point in the basin of attraction asymptotically converges. This formally defines the term "asymptotic" phase. The definition of the phase can be generalised in each of the basins of attraction of the co-existing limit cycles given by $x^{lc(1)}, x^{lc(2)}, ...$ Each of the phases $\phi(x^{lc(k)})$ is defined in its corresponding basin of attraction $\mathcal{B}(k)$, where k is the k^{th} limit cycle. The phases are not defined on the basin boundaries.

For systems exhibiting aperiodic dynamics, one can assign entities called protophases, which defines the set of points in the attractor $\mathcal{A}$ having almost similar phases. Protophases can be obtained using Hilbert transforms [20], mean first return times [2], by developing analytical equations for both the phase deviation and the probability density function of the phase deviation [21] and in terms of the slowest decaying modes of the Kolmogorov backward operator [22]. Recent studies by Imai *et. al* suggest that the adjustment of the scatter in phases could be carried out in accordance with the evolution of the non-phase variables for computing phases of chaotic oscillations [23]. Thus, the means of assigning an asymptotic phase to such attractors warrants studies in greater detail. Furthermore, the criteria that all trajectories cross the defined Poincaré section of the isophase in one direction does not strictly hold for stochastic oscillations. Noise could perturb the trajectory in the state space (in the case of additive noise) or alter the vector field (in the case of multiplicative noise), leading the trajectory to go back and forth in the state space while completing a cycle of oscillation. Nevertheless, if a return to the same surface happens after the trajectory performs a global loop *i.e.,* when the excursion is made through most regions of the state space that correspond to the underlying deterministic limit cycle, the oscillations and phases can be defined. The above notions have been discussed in detail for a pereiodic event driven stick-slip system.

This study focuses on development of algorithms for numerically computing isochronous limit sets and phase responses to perturbations of smooth and non-smooth oscillations of regular and aperiodic kind. Sec. 2 introduces definitions which will be used throughout the work. Sec. 3 discusses the phase response characteristics of a smooth automous oscillator while Sec. 4 discusses the autonomous case of a stick slip oscillator. The work ends with a summary of the salient outcomes of this study presented in Sec. 5.

2 Definitions

For any dynamical system described by $\dot{\mathbf{x}} = F(\mathbf{x}), \mathbf{x} \in \mathbb{R}^n$ for which limit cycles exist, there exists a point $\gamma(t)$ on the limit cycle Γ such that $\gamma(t) = \gamma(t+T)$. A phase can be assigned to this point along Γ. This can be done for all the points on the limit cycle. Here, the phase can be represented by a linearly increasing variable, cyclic in 2π, and can be mathematically expressed as $\phi(\mathbf{x})|_{\gamma(t)}, \phi \in [0, 2\pi)$, where $\mathbf{x}$ denotes the state variables of the dynamical system. The trajectory initiated at $\mathbf{x}$ asymptotically arrives in the proximity of $\gamma(t)$ and retains the oscillatory state on the limit cycle with the phase same as the point on the phase space labelled as $\gamma(t)$; see Fig. 1. Fig. 1(a) shows the trajectory on the limit cycle in blue; the point $\mathbf{x}$

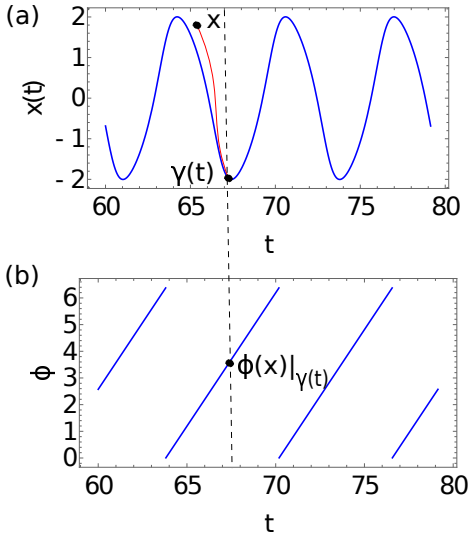

Fig. 1: Representative figure demonstrating (a) oscillations over the limit cycle Γ (in blue) and trajectory starting at an initial condition $\mathbf{x}$ (shown in red) that asymptotically converges to the limit cycle at $\gamma(t)$ (b) The phase variable mapped on the oscillations of the limit cycle $\Gamma(t)$ from $[0, 2\pi)$ (shown in blue). The phase mapped to the point $\mathbf{x}$ has been marked as $\phi(\mathbf{x})|_{\gamma(t)}$.

not on the limit cycle is the initial condition from which a numerical integration is initiated and the resultant trajectory is shown in red. The red trajectory converges to the limit cycle at $\gamma(t)$. Each point on the limit cycle can be mapped to a variable $\phi \in [0, 2\pi)$, which has been shown in Fig. 1(b). In the figure, one can observe three cycles of oscillations and correspondingly one can observe three diagonal lines. The phase associated with $\mathbf{x}$ is then the same phase as γ. The rate of change of phase $\mathrm{d}\phi/\mathrm{d}t\big|_{\Gamma}$ along the limit cycle attractor Γ denotes the frequency of oscillation ω. The collection of all these points in the basin of attraction $\mathcal{B}$ with the same asymptotic phase forms an isochron. Consider the system of differential equations

$$\dot{\mathbf{x}} = F(\mathbf{x}, t), \quad \mathbf{x} \in \mathbb{R}^n, \ (n \geq 2)$$

that possesses a hyperbolic periodic orbit $\gamma(t)$ of period T. Thus, $\forall \mathbf{x}$ in the basin of attraction of the orbit, there exists $\theta(x)$, such that

$$\lim_{\mathbf{x}\to\infty} |\mathbf{x}(t) - \gamma(t + \theta(\mathbf{x}))| = 0, \tag{1}$$

where $\mathbf{x}(t)$ is a solution of the dynamical system with an initial condition $\mathbf{x}_0$. $\theta(\mathbf{x})$ is the asymptotic or latent phase of $\mathbf{x}$. With this expression, one can assign a phase to each point in the basin of attraction of a periodic orbit so that $\theta(\mathbf{x})$ is a function on this domain, taking values in $[0, T)$. The collection of all points in the basin of attraction of γ with the same asymptotic phase is an isochron [15, 17]. A representative figure showing isochronous sets for a limit cycle can be seen in Fig. 2. The figure shows three isochronous sets in red dashed lines. An initial

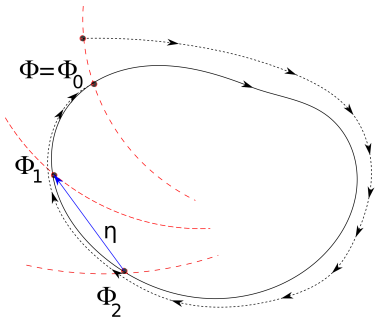

Fig. 2: A representative figure depicting a limit cycle, shown in black and corresponding 3 isochronous sets, shown in red. An initial condition lying on the isochron corresponding to ϕ_0 is shown to decay onto the limit cycle at ϕ_0 upon the evolution of the trajectory shown by black dashed lines. A perturbation η on a point over the limit cycle can shift the trajectory from one isochronous set to another after the effects of perturbations die out. The perturbed trajectory has not been shown.

condition lying on the isochron corresponding to ϕ_0 is shown to decay onto the limit cycle at ϕ_0 upon the evolution of the trajectory shown by black dashed lines. A perturbation η on a point over the limit cycle can shift the trajectory from one isochronous set to another after the effects of perturbations die out. The perturbed trajectory has not been shown. A perturbation η can make the trajectories jump from one isochronous set to another, leading to a transition in phase of oscillations, even while lying on the same attractor.

Now that the phase over the basin of attraction of limit cycle attractors is defined, one can examine the changes in dynamics for a given perturbation in accordance with the shift in the phase of oscillations. To examine the shift in ϕ given a perturbation, one studies the phase response curves. A phase response curve (PRC), also called a phase resetting curve, is measured numerically or experimentally by delivering a precisely timed perturbation to an oscillation and measuring the effect on the cycle period [24]. If the unperturbed period of the dynamical system is T_0 and if the cycle containing the perturbation completes one cycle of oscillation in time T_1, then the phase response curve, plotted as the relative

shift in phase against the amount of perturbation to the limit cycle, can be defined as $\Delta\phi = \frac{T_1 - T_0}{T_0}$. $\Delta\phi$ gives an insight into the advancement or retardation of phase, given a single perturbation to the trajectory at different points during its duration of oscillation. Thus, given a stable limit cycle $\Gamma(\mathbf{x}(\phi))$, one can determine the phase shift from ϕ to $\hat{\phi}$ due to the change of the states $\mathbf{x}(\phi) \longrightarrow \mathbf{x}(\hat{\phi}) = \mathbf{x}(\phi + k)$ simply by calculating the shift $\phi - \hat{\phi}$. This representation gives a sense of how long a trajectory spends in different regions of the state space.

Also known as phase resetting or phase sensitivity curve, PRC is a basic characteristic of a limit cycle oscillator [16,6] as it quantifies the transient change in the cycle period of an oscillator induced by a perturbation $p(t)$ as a function of the phase ϕ at which it is received. Mathematically, one can write

$$\dot{\phi} = \omega + Z(\phi)p(t) \tag{2}$$

where ω is the natural frequency of oscillation and $Z(\phi)$ is the oscillator's PRC. In order to study the PRC, the system is perturbed instantaneously with short and weak pulses at different values of the oscillator's phase. The subsequent variation for one or several oscillation periods is investigated for the evoked asymptotic phase shift. Fig. 3 shows a sample time history of a dynamical system as represented by the blue dashed line. The red line denotes the trajectory of the system when

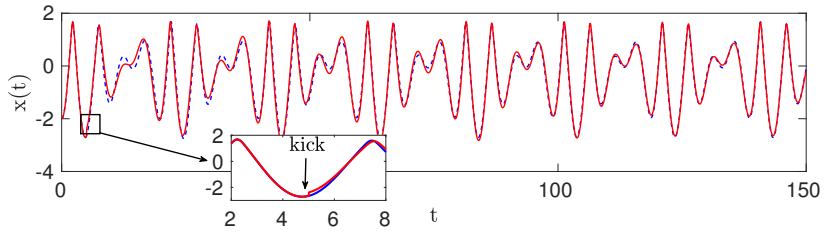

Fig. 3: The blue dashed line shows the system response. A small perturbation to the response is made at $t = 5$. It takes $\simeq 20$ cycles for the disturbance to die down and to converge onto the response time-history.

small perturbations are provided at discrete time steps as shown in the inset of the Fig. 3. It is seen that the soft impact oscillator system takes considerable number of cycles for the effect of the perturbations to die down even the smallest perturbation, provided as a reset at $x(t = 5)$ to $0.9\,x(t = 5)$.

The isochronous sets and phase response curves have been obtained for dynamical systems of smooth and non-smooth kinds. Autonomous and subsequently some non-autonomous problems are discussed in the following sections. The phase description of nonsmooth oscillators have been numerically obtained and are described in details. The subsequent sections aim towards shedding more clarity about picking an appropriate method for phase descriptions, given the conflicting methods discussed in literature for such suite of dynamical systems.

3 Smooth autonomous oscillator: Van der Pol oscillator

An autonomous deterministic Van der Pol oscillator is studied and the isochrons in its phase are plotted using the method of forward integration as follows. Starting from an initial condition $\mathbf{x}_0$ in the basin of attraction of a periodic attractor, the trajectory of the system is obtained by forward integration of the governing differential equation for time τ_1, say, until the following condition $|\Phi_\tau(\mathbf{x}_0) - \gamma(q)| < \epsilon$ for any $q \in [0, T)$ is satisfied. Here, $\Phi_\tau(\mathbf{x}_0)$ denotes the flow of the dynamical system starting from the initial condition $\mathbf{x}_0$ and evolved for time τ. Note that isochron of a deterministic system can be obtained using the method of backward integration [25].

3.1 Deterministic case

The governing equation of the autonomous Van der Pol oscillator is given by

$$\ddot{x} - \mu(1 - x^2)\dot{x} + x = 0. \tag{3}$$

The time histories for Eq. (3) with damping coefficient $\mu = 1$ and set of three distinct initial conditions $IC = \{[x_0, \dot{x}_0] : [0, 0.5], [-1, -0.75], [1, 0.75]\}$ are plotted in Fig. 4 (a). It is observed that after the transience dies out and the con-

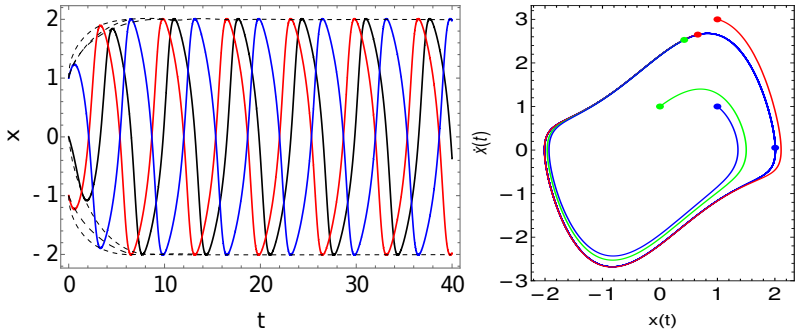

(a) (b)

Fig. 4: (a) Time histories of the Van der Pol oscillator starting from three different initial conditions are shown in blue, red and black solid lines. The black dashed lines connect the points of extreme amplitudes of oscillations. It is observed that the amplitude of the trajectories converge asymptotically after 1-2 cycles but have a significant phase difference in oscillations. (b) Phase plots for three different initial states, the initial states are shown as coloured circular points not on the attractor. The points on the limit cycle at which the convergence is achieved are shown as coloured dots on the attractor.

vergence is achieved, there are phase differences between the time histories. It can be verified from Fig. 4 (b) that the trajectories converge to the stable limit cycle Γ asymptotically, which is the unique attractor for the system for these

parameters. However they do so with different phases of oscillations $\phi(\mathbf{x})|_{\gamma(t)}$. Thus, the trajectories can be categorised into different isochronous sets. Mathematically, this can be expressed as the set of points in state space denoted by $I_i : \{\lim_{t\to\infty} |x(t) - \gamma(t-\phi)| = 0\}$, where $\phi \in [0, 2\pi)$ of $\Gamma(t)$, which is a periodic orbit of period T. Isochrons are shown as the loci represented as black lines in Fig. 5. The asymptotic phases have been represented as contours, mapped using a

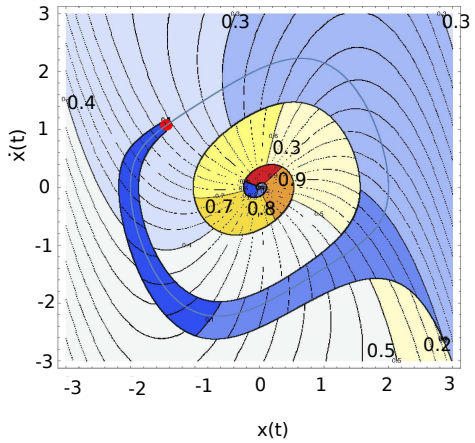

Fig. 5: Isochronous sets of the limit cycle oscillation of the Van der Pol oscillator. The isophases have been represented as contours coloured from blue to red assigned to the phase 0 to 2π respectively. The black solid lines in the figure denote the locus of initial conditions that end up at the same phase, *i.e* isochrons. $\phi = 0$ is denoted by the point on the limit cycle marked as red. Some of these isophases like 0.2, 0.3, 0.4, 0.5, 0.7, 0.8, 0.9 have been marked in the figure.

color map from blue to red for values ranging from 0 to 2π. The asymptotic phases $\phi \in [0, 2\pi)$ of trajectories when plotted against the initial conditions in the state space is seen in Fig. 6 (a). This figure gives a 3 dimensional representation of the phases. The notation ϕ_i denotes the phase of oscillation at time of evolution $t = i$. Since the value of $\phi_i = \phi_{i+2\pi}$, there appears to be a change of slope in the plane surface that the values describe.

The phase response curve, as defined in Sec. 2 has been computed using Xppaut [26]. Here, η is the intensity of the perturbation. To compute the PRC, the algorithm requires one to define a very high value of $x(t)$ as a threshold such that when there is a local maxima in the oscillation, the times of integration corresponding to these peaks can be numerically obtained. These peaks are considered as phase references. The shift in the duration of this peak value gives a measure of the phase response curve as defined in Sec. 2. The PRC for the Van der Pol oscillator has been presented in Fig. 6 (b). It can be seen that the PRC first reaches a minima and then gradually increases to a peak value before decreasing once again. This is because the phase varies between 0 and 2π. Although this method of defining a phase can be implemented for autonomous and event triggered spiking systems, as the transient durations are less and the perturbations often die out in a cou-

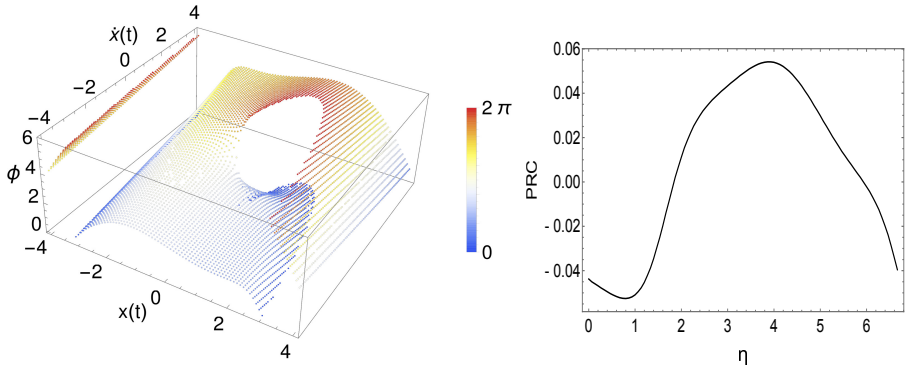

(a) (b)

Fig. 6: (a) Values of phases, reached asymptotically by the trajectories in the state space seen as a 3-dimensional plot. The plot folds back as $\phi_{t=0} = \phi_{t=2\pi}$ which explains the jump in the surface. (b) Phase response curve of a Van der Pol oscillator.

ple of cycles, there is an ambiguity in the definition of phase from the time the trajectory is perturbed to when it settles down on the attractor. Moreover, for non-autonomous systems, the time taken by the system to settle down asymptotically to the attractor following a perturbation is of the order of the time scale of the periods of the limit cycles. The fact that the above definition of phase gives a phase reference value even when the trajectory travels outside the stable limit cycle since it only takes care of local maxima, makes this method of computation of phase not directly suitable for non-autonomous systems.

3.2 Stochastic case

In the case of time evolution of the Van der Pol oscillator in the presence of continually applied noise, the equation of motion can be written down as

$$\ddot{x}(t) = (\mu(1 - x^2(t))\dot{x}(t) - x(t)) + n\lambda(\alpha, \sigma, \zeta, t) \tag{4}$$

where n denotes the intensity of the continuously applied noise represented by $\lambda(\alpha, \sigma, \zeta, t)$, governed by an Ornstein-Uhlenbeck process with process parameters given by α, σ and ξ denoting the mean, variance and the mean reversion speed respectively . The Ornstein-Uhlenbeck process can be written in the form $\dot{\lambda}(t) = -\theta\lambda + \sigma\eta(t)$, where $\eta(t)$ denotes white noise. In Eq. (4), the numerical values are taken to be $n = 0.3, \mu = 1$, α=0, σ=0.6 and $\xi = 0.1$.

The stochastic trajectory of the noisy system can be seen in Fig. 7(a). The blue trajectory depicts the response of a noisy Van der Pol oscillator that has been numerically integrated with a noise intensity of $n = 0.3$, while the red dots represent points strobed with the periodicity of the deterministic time period T. The three lines are three linear sections chosen to define the stochastic trajectory's proto-phases. It is observed that the noisy trajectory remains in the vicinity of the underlying deterministic limit cycle. To assign a notion of phase

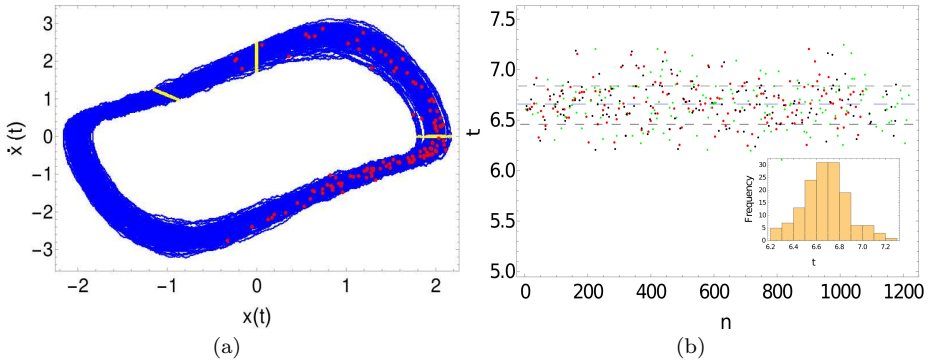

(a) (b)

Fig. 7: (a) The trajectory shown in blue is the response of the noisy Van der Pol oscillator numerically integrated with noise intensity of $n = 0.3$ and the red dots denote the Poincaré points strobed with the periodicity of the deterministic time period T. The three yellow lines correspond to three representative linear sections chosen to define proto-phases for the stochastic trajectory. (b) The mean return times of the three chosen proto-phases. n represents the number of full cycles the trajectory undergoes before reaching the defined sections and t represents the duration between these excursions. The blue dashed line represents the mean ($\mu(t)$) and the grey dashed lines are at standard deviation ($\sigma(t)$) apart from μ taken for all the points n. The inset shows the histogram of the mean return points.

for such an attractor, three linear observational sections were chosen arbitrarily along the limit cycle. These are shown as yellow lines transverse to the noisy limit cycle trajectories shown in Fig. 7(a). The sections satisfied the equations- $\Sigma_1 : x(t) = 0; \Sigma_2 : \dot{x}(t) = 0; \Sigma_3 : x(t) + \dot{x}(t) = 0.1, \dot{x}(t) > 0$. The return times of the trajectory to these sections, averaged over 1200 cycles, have been plotted in Fig. 7 (b). The time period T of the deterministic limit cycle was computed to be 6.6632. The red points in Fig. 7(b) denote the states on the trajectory with exact same return times. However, these are scattered and as it can be seen, no proper smooth line can be described over these points. One can always approximate these points of equal return with a higher order polynomial and define that as the system's isophase. The observational sections considered have "almost similar" return times with bounded variances and can be thus considered as individual estimates for isophases. Multiple such classes of isophases can thus be constructed based on the order of interpolation and the analytical formulation that satisfies the set of isophases over the whole trajectory. There are two conclusions from this observation. First, the isophases can be constructed in many ways [2] and that these defined smooth isophases will not have constant return times. An optimal isophase is the one where the variance is bounded and is defined for the specific problem under consideration. For any state j in the state space, the first time the trajectory passes a defined "almost-isophase" (also termed as protophase) can be given by the expression $T_j = \inf\{\mathrm{n} \geq 1; \mathbf{x}_\mathrm{n} = \mathrm{j}\}$. The expected or mean first return time to this section can be given by $E(T_j|\mathbf{x}_0) = j$. Since, the mean return times to the defined linear protophases are accurate to a significant number of decimal places, here 2, to the underlying known deterministic cycle, the assumed

sections can be considered as acceptable protophases for the stochastic limit cycle attractor. The phase of any other point which does not lie on the limit cycle can be described by the isophase that contains the final point on the state space after elapsed time τ, decided according to the problem under study [6]. Thus, a basin of isophases for the noisy case can be constructed. One can then have segments of isophases within each stochastic basin of attraction. For a given τ and a well defined isochronous set, an isochron for each initial condition is uniquely defined.

4 Non-smooth oscillators

Next, the focus is on describing a notion of phase of oscillations for limit cycle attractors that have components of sudden jumps or discontinuities in oscillations. This phenomena is observed in a suite of dynamical systems governed by n-dimensional piecewise smooth ODEs of the form $\dot{\mathbf{x}} = f_n(\mathbf{x}), \mathbf{x} \in S_n, n \in \mathcal{I}$. The state space is partitioned into regions $S_1, ..., S_m \subset \mathbb{R}^n$ and the boundaries of the partitions of S_n are assumed to be smooth $(n-1)$ switching manifolds. The discontinuity can occur in one of the state variables governing the system or their derivatives. Two examples of non-smooth systems have been taken up for these studies, namely the stick-slip belt friction model and the piece-wise smooth impact oscillator model.

4.1 Belt friction model

The self-excited mechanical system comprises of a block of mass m, supported by a moving belt, which is connected to a fixed support by a linear elastic spring of stiffness k. The contact surface between the mass and the surface is rough and thus a friction force is exerted by the belt on the mass. Energy is continually introduced to the system via the motion of the belt which is moving at a constant speed v while the dynamic friction force dissipates energy. These lead to a mechanical system undergoing self-sustained oscillations [27]. A schematic of the system is presented in Fig. 8. There are vibrations with stick and slip occurrences.

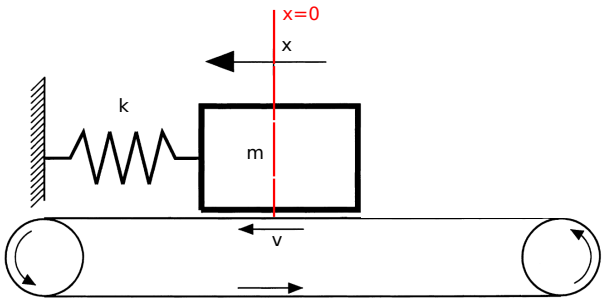

Fig. 8: Schematic of a single degree of freedom autonomous dry friction oscillator of mass m, moving as the belt slides with a constant velocity v.

The sticking occurs when the velocity of the oscillator is same as the velocity of the conveyor belt moving the oscillator, *i.e.,* they move along together. All the other occurrences are denoted as the slip kind. In the stick mode, the frictional force is a constraining force resisting motion whereas in the slip mode frictional force acts as an applied force that resists the existing motion. In such systems, the stick motion is considered uniform since the oscillator moves with the belt at the same velocity. Modelling the dry friction phenomena accurately is a difficult task as no single model can predict the dynamical behaviour accurately. Different friction models have been developed in order to understand the basic dynamical phenomena associated with the dissipation due to friction in accordance with experimental observations. In the problem under consideration, the frictional force experienced by the system is taken to be a culmination of different friction models. The model incorporates four types of friction: viscous, Coulomb, Stribeck, and static. Viscous friction is proportional to the relative velocity and is given by

$$F_v = -\alpha(\dot{x}(t) - v). \tag{5}$$

Given a slight displacement from the equilibrium position, the block quickly settles down to a stable position. The coulomb friction is proportional to the sign of relative velocity and is expressed as

$$F_c = \beta\,\mathrm{sgn}(\dot{x}(t) - v), \tag{6}$$

where

$$\mathrm{sgn}(x) = \begin{cases} -1, & x \leq 0, \\ 0, & x = 0, \\ 1, & x > 0. \end{cases} \tag{7}$$

Here, Coulomb friction models the frictional force that leads to the initial sticking of the block to the belt before it slides. In the Stribeck friction model, the frictional force is given by

$$F_s = \gamma\,\mathrm{sgn}(\dot{x}(t) - v)\mathrm{e}^{(-2|\dot{x}(t)-v|)}. \tag{8}$$

Static friction, on the other hand has an overall effect of holding the block in place until the spring force exceeds the value of μ, which depends on the roughness of the surfaces. Thus, the overall equation of motion of the system can be given as

$$m\ddot{x} = \begin{cases} k(1-x) + F_s + F_c + F_v, & \dot{x}(t) \neq v \\ v, & \dot{x} = v\,,\ [k(1-x)]^2 < \mu^2 \\ k(1-x) + F_s + F_c + F_v, & \dot{x} = v\,,\ [k(1-x)]^2 \geq \mu^2. \end{cases} \tag{9}$$

For the sake of computations the numerical values for the parameters in Eq. (9) are taken to be $\alpha = -0.3, \beta = -25, \gamma = -0.3$. The value of m is taken as 1, $k = 1000$, speed of the belt $v = 0.1, \mu = 100$. This system falls under a broad class of nonsmooth dynamical systems also referred to in the literature as Filippov systems [27]. The numerical modelling of Filippov systems involves an additional rule governing the sliding motion when $\dot{x}$ denoting the discontinuity boundary takes the value of v. The equations of motion can be integrated numerically using the event driven model of representation. The block repeatedly sticks to the belt due to frictional forces and then slips back due to the spring force.

4.1.1 Periodic oscillations

When the set of ODEs in Eq. 9 are numerically integrated, a unique period-1 limit cycle is observed. During its evolution, the trajectory sticks to the belt with a constant speed of $v = 0.1$; see Fig. 9. Three trajectories emanating from

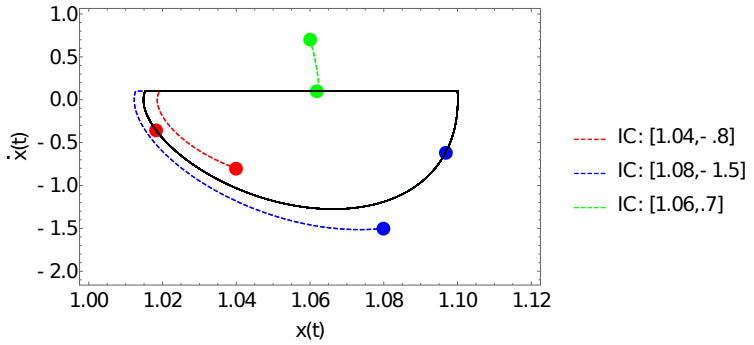

Fig. 9: Figure showing three different initial states, with coloured points not on the attractor and end states when they reach the attractor, with coloured points on the attractor.

different initial conditions are shown in the figure. The corresponding points on the trajectory when it first ends up at the limit cycle has also been highlighted. To map each segment of the limit cycle to a unique phase, the time-period T of the autonomous limit cycle is first numerically obtained. To do so, a point on the limit cycle is chosen, here $\{1.04, 0.1\}$. The times at which the trajectory crosses this point are noted for 100 cycles with the help of event detection algorithms. Once these times of crossing are noted, the initial transient values are dropped and the mean of the remaining observables is considered as the time-period. The values of state variables after each elapsed time $T/5000$ is computed. These states are then mapped in a one-to-one fashion to phases corresponding to $[0, 2\pi)$. The fraction of time in a cycle for which this period 1 attractor stays in its stick phase, *i.e.,* when $\dot{x}(t) = 0.1$, in proportion to the time it slips and makes an excursion along the state space is computed. Time steps are taken in very small increments of $\delta t = 10^{-6}$ while computing this entity. The ratio is computed to be $\simeq 87.32\%$. Thus, the stick phase dominates over the limit cycle, as seen in Fig. 9.

To compute the response to perturbations along different phases of this limit cycle, initially the states on the limit cycle have been mapped to the phase variable $\phi \in [0, 2\pi)$. To do so, a reference trajectory is taken beginning with the initial condition $x_0 = 1, \dot{x}_0 = 1$. The dynamics is traced till $t = 200$. It was observed that the transient dynamics of the trajectory dies down by $t = 200$. The state of the system at $t = 200$ is therefore taken to be the reference state, which is mapped to $\phi = 0$. The corresponding time is denoted as t_{ref}. The subsequent points on the limit cycle are mapped from 0 to 2π until the oscillation completes one full cycle at time $t = t_{ref} + T$. The trajectories of the system starting with certain initial conditions is then monitored on the state space. The phase of oscillation of the trajectory after $50 \times t_{ref}$, which is well beyond the time period in which the

transients die out, is computed by obtaining the Euclidean distance between the values of state variables x and $\dot{x}$ with the reference trajectory with a tolerance of 10^{-4} and then mapping it back to the phase variable as defined earlier. This is done for all trajectories in the basin of attraction $\mathcal{B}$, which in this case spans the state space. The phases of oscillations numerically obtained from the asymptotically converged trajectories have been plotted against initial conditions and can be seen in Fig. 10. The surface, unlike the case of the Van der Pol oscillator is seen to have

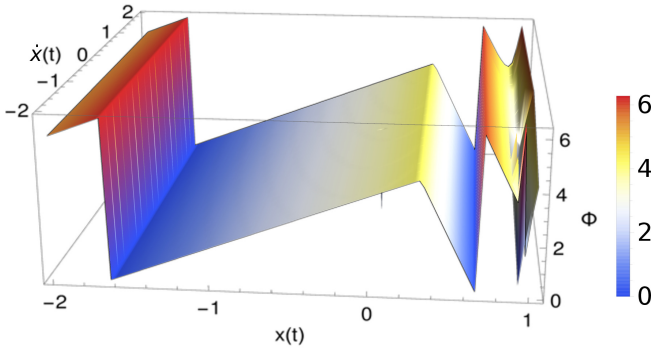

Fig. 10: Phase of oscillation of the trajectory beginning an initial condition in $x-\dot{x}$, observed as a 3-dimensional plot. The surface has multiple sharp edges, denoting abrupt transitions in phases.

relatively abrupt transitions in phases attained by the trajectories. This is due to the fact that the time the trajectory spends in the slip phase is significantly lesser as compared to the stick phase of its oscillation, even though the system makes a larger excursion in the phase space during its slip state. Thus, most trajectories are mapped to the stick state, which is mapped to the phase change that is gradual. The phase change is abrupt when the dynamics is mapped to the phases where slipping occurs, for instance at $x(t) = 0.23$ and near $x(t) = 1$.

Now, the behaviour of the trajectory dislodged by a perturbation with a magnitude of η is studied. A perturbation is given to the evolving trajectory at $t = t_{ref} + \tau$. This displaces the state variable x as $x(t) \to \eta \times x(t)$. When $t = 5$, say, one can observe that beyond the small transients the trajectory asyptotically converges to the attractor with shifts in phase depending on the intensity of the perturbation η; see Fig. 11(a). Thus, a phase response curve can be drawn for the following responses as a function of the intensity of the displacement. The nature of the phase response curve is linear and repeats in 2π every η value of $\simeq 0.105$, as seen in Fig. 11(b).

5 Conclusions

The isochronous sets and phase responses of smooth and non-smooth dynamical systems pertaining to mechanical oscillators have been analysed. When a limit cycle attractor has periodicity more than unity, the existing metrics for defining

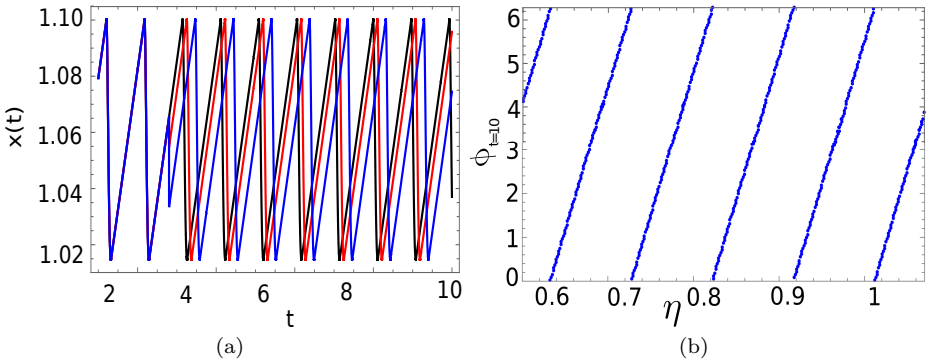

(a) (b)

Fig. 11: (a) Single non-small perturbations defined by $x(t) \to \eta \times x(t)$ of intensities η= 0.97 in blue, η= 0.96 in red, η= 0.92 in black at $t = 3$ leads to the shift in phase of the trajectory. (b) Phase of oscillations at $t = 10$ when the trajectories are dislodged with a perturbation at $t = 5$ of magnitude $\eta \in [0.6, 1.07]$, leading to shifts in phase of oscillations.

phase tend to assign the same phase to multiple points on the attractor. This study focussed on developing an approach for defining protophase along the lines discussed in [2]. Limit cycles with instantaneous reversals, sliding discontinuities and piece-wise smooth kind of discontinuities as well as aperiodic oscillations were analyzed for their phase responses. For noisy oscillations, the average period of oscillations have been computed and almost-isophases have been fit according to a smoothness constrained optimization problem. These results can have applications in defining synchronization properties of oscillators. Further studies can be focused on noise perturbed chaotic attractors, quasiperiodic attractors and other dynamically observed suite of attractors of the aperiodic kind.

Declarations

Funding: S Gupta thanks IIT Madras for partial funding from the CoE project no SP20210777DRMHRDDIR117.
Conflicts of interest/Competing interests: The authors declare that they have no conflict of interest.
Availability of data and material: Relevant data will be shared on request.
Code availability: Relevant codes will be shared on request.

References

1. Osinga, H.M., Moehlis, J.: Continuation-based computation of Global Isochrons. SIAM Journal on Applied Dynamical Systems. **9**, 1201–1228 (2010).
2. Schwabedal, J.T., Pikovsky, A., Kralemann, B., Rosenblum, M.: Optimal phase description of chaotic oscillators. Physical Review E. **85**, (2012).
3. Strogatz, S.H.: From Kuramoto to crawford: Exploring the onset of synchronization in populations of coupled oscillators. Physica D: Nonlinear Phenomena. **143**, 1–20 (2000).
4. Winfree, A.T.: The geometry of Biological Time. Springer, New York (2011).

5. Pikovsky, A.S., Rosenblum, M.G.: Phase synchronization of regular and chaotic self-sustained oscillators. Synchronization: Theory and Application. **187–219** (2003).
6. Schwabedal, J.T., Pikovsky, A.: Phase description of stochastic oscillations. Physical Review Letters. **110**, (2013).
7. Lai, Y.-C., Ye, N.: Recent developments in chaotic time series analysis. International Journal of Bifurcation and Chaos. **13**, 1383–1422 (2003).
8. Norden E, H.: Computer implemented empirical mode decomposition method, apparatus and article of manufacture, Google Patents, US Patent **5,983,162** (1999).
9. Cao, A., Lindner, B., Thomas, P.J.: A partial differential equation for the mean–return-time phase of planar stochastic oscillators. SIAM Journal on Applied Mathematics. **80**, 422–447 (2020).
10. Pikovsky, A.: Comment on "Asymptotic phase for stochastic oscillators." Physical Review Letters. **115**, (2015).
11. Thomas, P.J., Lindner, B.: Thomas and Lindner reply: Physical Review Letters. **115** (2015).
12. Schwabedal, J.T.C., Pikovsky, A.: Effective phase description of noise-perturbed and noise-induced oscillations. The European Physical Journal Special Topics. **187**, 63–76 (2010).
13. Efimov, D., Sacre, P., Sepulchre, R.: Controlling the phase of an oscillator: A phase response curve approach. Proceedings of the 48h IEEE Conference on Decision and Control (CDC) held jointly with 2009 28th Chinese Control Conference. (2009).
14. Bagheri, N., Stelling, J., Doyle, F.J.: Circadian phase entrainmentvia nonlinear model predictive control. International Journal of Robust and Nonlinear Control. **17**, 1555–1571 (2007).
15. Guckenheimer, J.: Isochrons and phaseless sets. Journal of Mathematical Biology. **1**, 259–273 (1975).
16. Glass, L., Mackey, M.C.: From clocks to Chaos: The rhythms of life. Princeton University Press, Princeton (N.J.) (1988).
17. Brown, E., Moehlis, J., Holmes, P.: On the phase reduction and response dynamics of neural oscillator populations. Neural Computation. **16**, 673–715 (2004).
18. Awrejcewicz, J., Kurpa, L., Mazur, O.: Dynamical instability of laminated plates with external cutout. International Journal of Non-Linear Mechanics. **81**, 103–114 (2016).
19. Kuramoto, Y., Nakao, H.: On the concept of dynamical reduction: The case of coupled oscillators. Philosophical Transactions of the Royal Society A: Mathematical, Physical and Engineering Sciences. **377**, 20190041 (2019).
20. Freund, J.A., Schimansky-Geier, L., Hänggi, P.: Frequency and phase synchronization in stochastic systems. Chaos: An Interdisciplinary Journal of Nonlinear Science. **13**, 225–238 (2003).
21. Bonnin, M., Corinto, F.: Phase noise and noise induced frequency shift in stochastic nonlinear oscillators. IEEE Transactions on Circuits and Systems I: Regular Papers. **60**, 2104–2115 (2013).
22. Thomas, P.J., Lindner, B.: Asymptotic phase for Stochastic Oscillators. Physical Review Letters. **113**, (2014).
23. Imai, T., Suetani, H., Aoyagi, T.: On the phase description of chaotic oscillators. Journal of the Physical Society of Japan. **91**, (2022).
24. Canavier, C.C.: Phase response curve, http://www.scholarpedia.org/article/Phase_response_curve.
25. Josic, K., Shea-Brown, E.T., Moehlis, J.: Isochron, http://www.scholarpedia.org/article/Isochron.
26. Ermentrout, B.: Simulating, analyzing, and animating dynamical systems: A guide to XPPAUT for researchers and students. Society for Industrial and Applied Mathematics, Philadelphia (2002).
27. Galvanetto, U.: Non-linear dynamics of multiple friction oscillators. Computer Methods in Applied Mechanics and Engineering. **178**, 291–306 (1999).